Aerosol and Air Quality Research, 19: 2585–2596, 2019

ISSN: 1680-8584 print / 2071-1409 online
doi: 10.4209/aaqr.2018.08.0306

Effects of Acoustic and Pulse Corona Discharge Coupling Field on Agglomeration and Removal of Coal-fired Fine Particles

Mingchun He, Zhongyang Luo*, Mengshi Lu, Shuxin Liu, Mengxiang Fang

State Key Laboratory of Clean Energy Utilization, Zhejiang University, Hangzhou 310027, China

ABSTRACT

Fine particles from coal-fired power plants are harmful to human health and the atmosphere. Traditional electrostatic precipitators (ESPs) exhibit low efficiency in removing such particles. By contrast, pulsed corona discharge and high-intensity acoustic waves are effective pretreatment methods by which fine particles can be agglomerated into larger particles. Coupling these two fields can enhance the agglomeration process. In this study, a laboratory-scale experimental setup was established to investigate the agglomeration and efficient removal of fine particles. According to the results, application of the coupling field increased the median particle diameter (D_{50}) and agglomeration ratio (R_{ae}) compared with use of a single field. Under the coupling field approach, when pulse input and acoustic wave parameters were 55 kV–100 Hz and 143 dB–1600 Hz, respectively, D_{50} and R_{ae} reached 73.28 μm and 9.18, respectively, and numerous fine particles agglomerated into large particles that could be removed using an ESP. Furthermore, the overall efficiency of removing fine particles increased to 98.3% under optimal conditions compared with the 80.7% efficiency exhibited when pretreatment was not applied.

Keywords: Coupling field; Agglomeration ratio; Particulate matter; Electrostatic precipitator.

INTRODUCTION

With the rapid development of China's social economy, energy consumption has generated inhalable particles comprising heavy metals and toxic substances. These particles have become primary atmospheric and indoor environmental pollutants, and they severely threaten human health and air quality (Xu *et al*., 2014; Wang *et al.*, 2016; Liao *et al.*, 2018). In China, haze caused by fine particulate matter is severe (Zhou *et al*., 2012). Conventional ESPs exhibit low collection efficiencies for submicron particles, because fine particles are difficult to charge (Le *et al.*, 2013). Thus, the available technologies are insufficient for environmental protection and must be upgraded.

Fine particle agglomeration technology has been increasingly discussed as an effective tool for particle pretreatment to enlarge fine particle size. Relevant strategies include electrical agglomeration (Matsoukas, 1997), acoustic agglomeration (Hoffmann, 2000), chemical agglomeration (Liu *et al*., 2009), and water vapor condensation (Chen *et al*., 2002), In acoustic agglomeration, high-intensity sound waves induce relative motion and frequent collision among particles of various sizes to achieve agglomeration. Many experimental studies and theoretical analyses have addressed this strategy (Liu *et al*., 2009; Zhang *et al*., 2012). Wang *et al*. (2011) conducted an experiment to compare the effect of acoustic agglomeration using high-frequency acoustic waves with that using low-frequency acoustic wave. The results revealed that low-frequency acoustic waves induced more efficient agglomeration of fly ash particles than the high-frequency acoustic waves. Zhou *et al*. (2016) conducted an experiment on the enhancement of the particle removal efficiency of acoustic agglomeration; the results showed that use of an acoustic wave field improved the removal efficiency of bag filters from 91.29% to 99.19% and that of ESP from 89.05% to 99.28%. Pulse corona discharge can generate amounts of high-energy free electrons, which ionize gas molecules in the process of moving to the anode (Xu *et al*., 2009). Because of the migration rate difference between positive ions and electrons, pulse corona discharge is mainly a bipolar charging process, whereas DC corona discharge is mainly an unipolar charging process (Jiang *et al*., 2015). Liao *et al.* (2018) conducted an experimental study with the aim of improving particle removal performance using an enhanced unipolar pre-charger. The results revealed that removal efficiency was 12.1%–15.9% greater when the pre-charger was used, as compared with the results obtained without the pre-charger.

Experimental studies have also examined particle agglomeration in coupling fields. Zhang *et al*. (2017)

* Corresponding author.
Tel.: +86-571-87952440; Fax: +86-571-87951616
E-mail address: zyluo@zju.edu.cn

investigated acoustic agglomeration in the presence of liquid drops, and discovered that water spray droplets enhanced acoustic agglomeration by up to 55%. Yan *et al*. (2016) conducted an experimental study on the coupling field of acoustic wave and vapor condensation, and reported that particle removal efficiency was significantly increased by the coupled field, reaching 53%–80% when sound pressure level (SPL) was 150 dB and the supersaturation degree was 1.2. Chen *et al*. (2017) investigated a coupling field enhanced by spray droplets, and the results revealed that particle penetration efficiency increased up to 10% with this enhancement of the coupling field. Most studies have focused on reducing particles of 0–10 μm, particles larger than 10 μm growth rate has not been investigated. In the present study, the coupling field of pulse corona discharge and acoustic wave was applied in an agglomeration chamber, and a laser particle analyzer was used to monitor changes in particle sizes. A conventional ESP placed at the outlet of the agglomeration chamber was used to collect particles. This experiment investigated the effect of using a coupling field compared with a single field, in terms of median particle diameter change and removal efficiency.

EXPERIMENTAL SETUP AND METHODOLOGY

In this experiment, the feeding system comprised a SAG 410/L aerosol generator, with a flow rate of 1–264 g h^{-1} (Fig. 1). The agglomeration chamber was a vertical cuboid fabricated from polymethyl methacrylate (PMMA). The height of the chamber was 1200 mm, and the side length was 120 mm. Inside the chamber, four stainless steel wire electrodes were located every 100 mm and each had a diameter of 2 mm and a length of 80 mm. Additionally, the chamber contained two discharge plates for the production of pulse corona discharges. Sound-absorbing foam was used in the chamber to reduce the reflection of sound waves. The acoustic wave system comprised a SFG-1013 signal generator, YF-513 compression driver, and a QSC RMX2450 power amplifier, which were used to set acoustic frequencies between 180 and 5500 Hz. Based on the consideration that energy input breaks aggregates into pieces, SPLs between 135 and 143 dB were chosen in this study. These SPLs have been proven effective in other studies (Liu *et al.*, 2009; Wang *et al*., 2011). The pulsed corona discharge system involved a narrow-pulse HV generator, Tektronix TCP0150 current probe, Tektronix DPO4034 digital oscilloscope, and P150-GL HV probe. The system was used to control input parameters and acquire the I–V curve. Subsequently, particles flowed through the agglomeration chamber, and particle size distribution (PSD_1) was captured using a DP-02 laser particle size analyzer. An electrical low pressure impactor (ELPI) was placed after the ESP to measure the particle concentration and particle size distribution between 0 and 10 μm (PSD_2). A two-stage diluter was used to ensure that the flow rate to the ELPI was 10 m^3 h^{-1}. The ESP was wire-plated and used a negative direct current (DC) power supply.

Jiaxing coal-fired plant fly ash particles were used in this experiment, and they were mixed before being released into the agglomeration chamber. A DP-02 laser particle size analyzer was used to ensure that a laser beam could penetrate the bottom part of the agglomeration chamber. In this study, the ELPI measurement range was less than 10 μm, but a substantial proportion of the agglomerated particles was larger than 10 μm. The DP-02 laser particle size analyzer was utilized to measure the size change of the agglomerated particles to verify the effect of the coupling field.

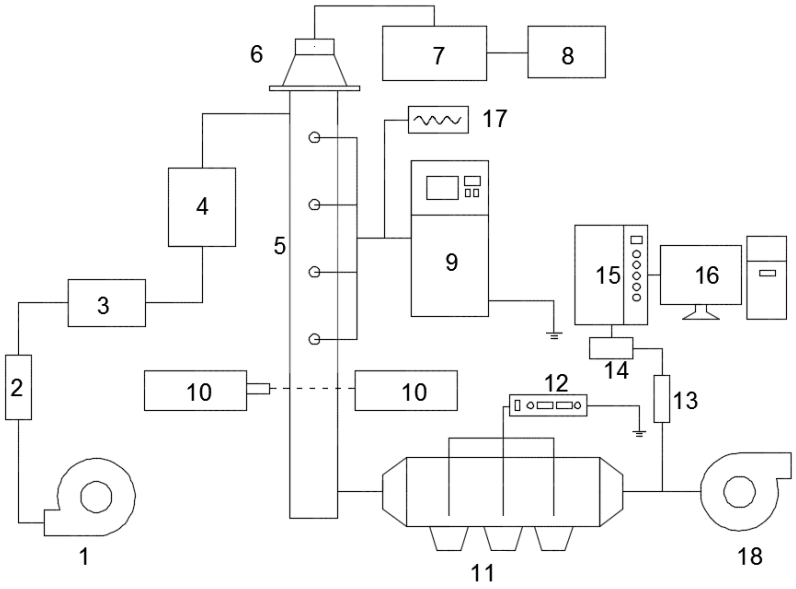

1. Blower, 2. Flowmeter, 3. feeding system, 4. buffer tank, 5. agglomeration chamber, 6. compression driver, 7. power amplifier, 8. signal generator, 9. narrow-pulse high-voltage generator, 10. DP-02 laser particle analyzer, 11. ESP, 12. high voltage DC power supply, 13. electrostatic neutralizer, 14. Diluter, 15. ELPI, 16. Computer 17. oscilloscope, 18. vacuum pump

Fig. 1. Schematic of experimental setup.

THEORETICAL ANALYSIS

Particle charges, particle collisions, and particle–gas interactions are involved in the processes of particle agglomeration and removal. Thus, when particles flow through an agglomeration chamber, multiple forces may act upon them, such as Coulomb force between charged particles, viscous Stokes' drag force, gravitational force, inertial force, and buoyancy force. The mechanism resulting from these mutually influential forces is complex.

Pulse Corona Discharge

High-voltage pulse discharge differed from negative DC discharge; the high-voltage discharge process comprised two stages: a discharge period and an intercritical period. In this study, high-voltage generator frequency ranged from 100 to 300 Hz, but the pulse width was only 300–400 ns, and the intercritical period was much longer than the discharge period. Discharge occurred in formed streamer-channels in which numerous high-energy free electrons and ions coexisted. The high-energy free electrons migrated more rapidly than did the ions, and in the agglomeration chamber, the concentrations of positive and negative ions were extremely unbalanced (McAdams, 2007). Thus, the discharge period, mainly involved the charging of fine particles by high-energy free electrons. After the discharge period, numerous ions remained in the reaction space. The number of negative ions was substantially lower than that of positive ions, and most of the negative ions were neutralized within a short period (McAdams, 2007). Thus, charges from positive ions were more prevalent on fine particles.

Based on the preceding analysis, during the discharge period, electron flux was solved to identify charge number (Liu and Kapadia, 1978; O'Hara *et al*., 1989):

$$\Pi\big|_r = -\mu_e N_e(r)E - D_e \nabla N_e(r) \tag{1}$$

where μ_e is the migration rate of high-energy free electrons; $N_e(r)$ is the concentration of high-energy free electrons r away from the particle center; D_e is the diffusion coefficient of high-energy free electrons; and $\nabla N_e(r)$ is the concentration gradient of high-energy free electrons r away from the particle center.

When electron flux is small, Einstein's equations should be introduced to solve Eq. (1), where the energy distribution of high-energy free electrons is assumed to conform to Maxwell distribution (Bates *et al.*, 1962):

$$KT_e = \frac{2}{3}X\left(\frac{D_e}{\mu_e}\right)e \tag{2}$$

where K is the Boltzmann constant; $K = 1.38 \times 10^{-23}$ J K^{-1}; T_e is the temperature of high-energy free electrons; X is a constant; and X = 3/2 when energy distribution of high-energy free electrons conforms to Maxwell distribution,

$$\ln N_{e(r)} = \frac{e\Phi_{(r)}}{KT_e} + A \tag{3}$$

where $\Phi_{(r)}$ is electric potential r away from the particle center; A is a constant; and the boundary conditions are $\Phi_{(r)} = 0$, $N_{e(r)} = N_{e0}$,

$$N_{e(r)} = N_{e0}\exp\left(\frac{-e\Phi_{(r)}}{KT_e}\right) \tag{4}$$

where N_{e0} is the original concentration of high-energy free electrons. If electron flux is large enough or the ratio of electric field intensity to gas molecular density is large enough, the energy distribution of high-energy free electrons deviates from Maxwell distribution; Eq. (4) is no longer applicable; and $\Phi_{(r)}$ refers to electric potential under the influence of particles' own charge and external electric field,

$$\Phi_{(r)} = \frac{-q_1}{4\pi\varepsilon_0 r} - \left[\frac{r}{R} - \left(\frac{\varepsilon-\varepsilon_0}{\varepsilon+2\varepsilon_0}\right)\frac{R^2}{r^2}\right]E_0 a\cos\theta \quad (r \geq R) \tag{5}$$

where q_1 is particle charge; r is the distance between a point in the reaction system and a particle center; ε is a particle's relative dielectric constant; ε_0 is the permittivity of vacuum; E_0 is the original electric field intensity in the reaction system; θ is the angle of a line between the particle center and a point r away from the particle center and the electric field line.

Eqs. (1), (4), and (5) indicate that high-energy free electron flux could be created on the surface of particles,

$$\frac{\mathrm{d}q_1}{\mathrm{d}t} = -2\pi e a^2 \int_{\theta=0}^{\theta=\pi} \Pi\big|_{r=a} \sin\theta \mathrm{d}\theta \tag{6}$$

To solve Eq. (6), the boundary condition ($\nabla N_e(r = R) = 0$) should be applied, because electron density distribution conforms to Boltzmann distribution, and continuous electron distribution occurs around particles. Thus, solution is as follows:

$$q_1 = \frac{4\pi\varepsilon_0 RKT_e}{e}\ln\left[1 + \frac{N_{e0}Re^2\mu_e E_0 t}{2\varepsilon_0 KT_e}\left(\frac{e^{\alpha} - e^{-\alpha}}{\alpha}\right)\right] \tag{7}$$

$$\alpha = \frac{-3eE_0 R}{\left(\frac{\varepsilon}{\varepsilon_0} + 2\right)KT_e} \tag{8}$$

With the increase of electric field intensity, particles receive more charges. Similarly, after the discharge period, particles capture positive ions and become positively charged:

$$q_2 = \frac{4\pi\varepsilon_0 RKT}{e}\cdot\ln\left[1 + \exp\left(-\frac{e^2 B}{RKT}\right)\frac{\pi u_i e^2 R N_{i0} t}{KT}\right] \tag{9}$$

where B is a constant related to R, ε, and ε_0.

Due to the opposite charges present among particles

during the discharge period, Coulomb force exists in the agglomeration chamber:

$$F_C = \frac{q_1 q_2}{4\pi\varepsilon R^2} \tag{10}$$

According to studies on fine particle charges (Jiang *et al.*, 2015; Xu *et al.*, 2009), small and large particles exhibit opposite charges and attract each other, resulting in the formation of numerous aggregates.

Acoustic Wave Field

Acoustic wave is a promising pretreatment method for achieving particle agglomeration. In an intensive acoustic wave field, particles are entrained by gas media. Orthokinetic interaction plays a key role in the acoustic agglomeration process (Sheng and Shen, 2007). In the orthokinetic interaction process, an acoustic wave causes air medium vibration; because of the viscosity of the gas, particles in the aerosol vibrate in response. Large particles with large inertia are not readily carried by gas while small particles are easy to be carried. Different vibration amplitudes result in relative motion and collision between particles of different sizes, and the entrainment coefficient μ_p can be defined as follows (Zhou *et al*., 2017):

$$\mu_p = \frac{u_p}{u_g} \tag{11}$$

Several forces are present in the acoustic field, namely pressure gradient force, viscous Stokes' drag force, and the force required for fluid acceleration near the particles. In this study, particle motion was limited within Stokes flow (Re < 1), and only viscous Stokes' drag force was considered:

$$F_p = \frac{6\pi\mu_g R(u_g - u_p)}{c_c} \tag{12}$$

where μ_g is the dynamic viscosity of gas; R is particle radius; u_g is the velocity of gas; u_p is the velocity of particles; and C_c is Cunningham correction factor (Fan *et al*., 2013).

Entrained particles in gas medium vibrate and lag behind the gas. The particle motion equation can be expressed as follows:

$$u_g = u_0 \sin \omega t \tag{13}$$

The velocity of particles can then be simplified as follows,

$$u_p = \frac{u_0 \sin(\omega t - \varphi)}{\sqrt{1+\omega^2\tau^2}} \tag{14}$$

where τ is the relaxation time of particles, u_0 is the velocity amplitude of gas medium; ω is angular frequency; and $\omega = 2\pi f$,

$$\tau = \frac{2\rho R^2 C_c}{9\mu_g} \tag{15}$$

where f is the acoustic wave frequency. φ is the phase difference between gas medium and particles, so the entrainment coefficient μ_p can be de represented as follows:

$$\mu_p = \frac{1}{\sqrt{1+\omega^2\tau^2}} = \frac{1}{\sqrt{1+4\pi^2 f^2 \tau^2}} = \cos\varphi \tag{16}$$

Fig. 2 presents the effects of particle size and acoustic wave frequency on the acoustic entrainment factor. The value of μ_p is between 0 and 1, and a larger entrainment factor signifies that particles are readily entrained by the gas medium. When μ_p reaches 1, the vibration amplitude of the particles and air medium is synchronized. By contrast, when μ_p is 0, particle motion is not affected by acoustic waves and remains vibrationless. Larger particles are easily entrained when acoustic wave frequency is low. Specific frequencies, correspond with specific entrainment factors. These factors can be utilized to prove the existence of optimal acoustic parameters for inducing relative movement and collision of particles with various diameters.

In the acoustic wave field, countless particles collide, and large particles are likely to be shattered by acoustic waves. Because of the existence of a pulse corona field, particles with various diameters receive opposite charges due to differences in charging mechanisms, and Coulomb force may cause them to adhere and aggregate into larger particles. Thus, the coupling effect increases the possibility of reunion and agglomeration. Application of ESP substantially increases the efficiency of small particle removal.

RESULTS AND DISCUSSION

In this study, fly ash particle was assumed to be a convex spherical particle. A DP-02 laser particle analyzer and ELPI were utilized to measure the particle agglomeration process and particle removal efficiency respectively. Studies have focused on measuring removal efficiency using ELPI. ELPI measurement range is less than 10 μm; thus, ELPI is insufficient for monitoring particles with larger diameters. In this study, DP-02 was selected to measure particle size change online. The particle size measuring mechanisms of ELPI and the DP-02 laser particle analyzer differ; ELPI data are based on aerodynamic size, whereas DP-02 data are based on optical particle size. As presented in Fig. 3, original particle size distribution PSD_1 (DP-02) was compared with transformed PSD_2 (ELPI) in the same coordinate system. The results show that the curves of the PSDs coincided; thus, the respective PSDs could be used to investigate agglomeration and removal efficiency.

In a DC electric field, I–V characteristic curve was used to analyze the power supply properties. A narrow-pulse

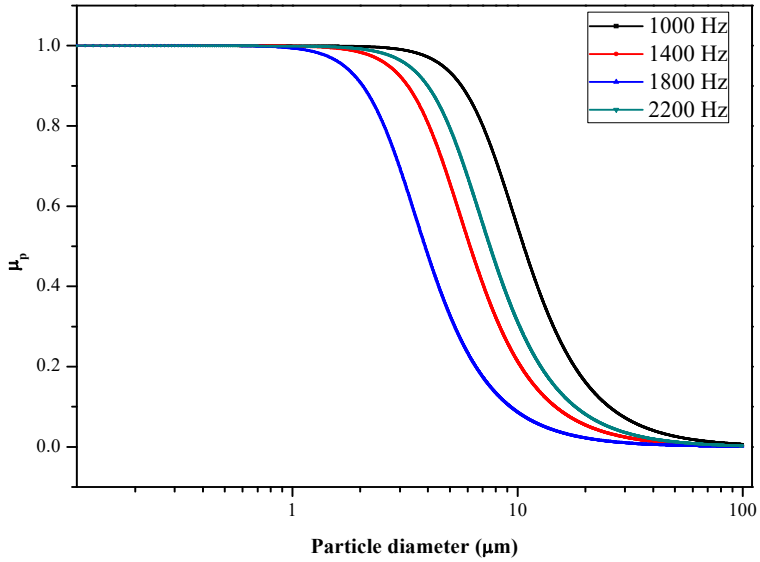

Fig. 2. Relationship between the entrainment factor and particle diameter at various acoustic frequencies.

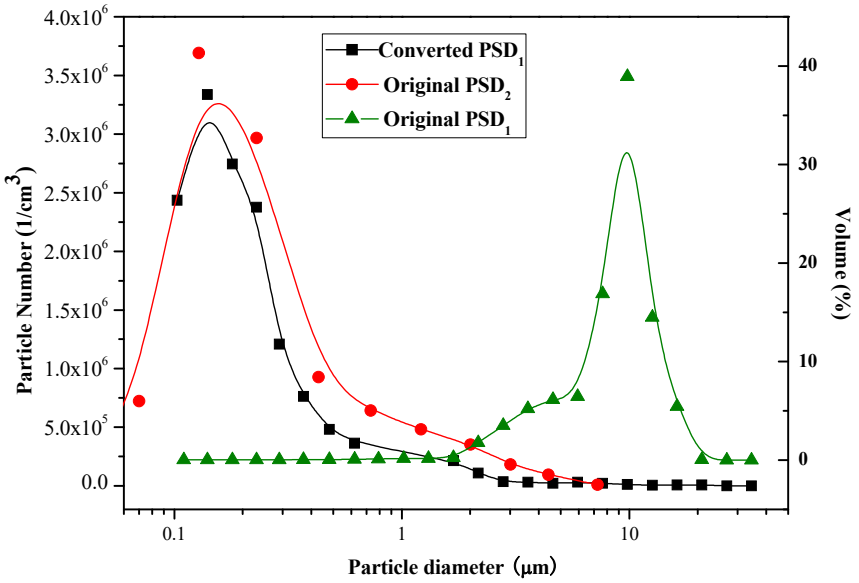

Fig. 3. Original particle size distribution of the ash.

HV generator was used as an intermittent discharge device. Consideration of energy input was required. Energy input reflects electron and ion density changes and reaction processes, as well as migration rate. Single pulse energy was introduced to describe pulsed corona discharge energy consumption. Pulse corona discharge frequency ranged from 100 to 300 Hz. Fig. 4 illustrates the pulsed corona discharge characteristics. When input voltage increased, single pulse energy will increased; in other words, more energy was injected into the reaction space, and 100 Hz single pulse energy was the largest, followed by 200 and 300 Hz.

Effects of Pulse Corona Discharge on the Agglomeration of Fine Particles

The purpose of this experiment was to verify the influence of pulse corona discharge on PSD_1. The results are as presented in Fig. 5(a). New peak values in the pulse field were noted, and the corresponding median particle size increased. When the voltage was 35 and 45 kV, the new peak value after agglomeration was approximately 30 μm, and the volume proportions of 27-μm particles reached 4.46% and 11.84%, respectively. Most small particles remained. When the pulse voltage increased to 55 kV, the volume proportion of small particles dramatically decreased. The proportion of 9.82-μm particles dropped to 31.28%, and the proportion of 27-μm particles increased to 25.96%. When the pulse frequency was 100 or 200 Hz, new peaks appeared at 155 μm, and the peak values were 6.29% and 4.01%, respectively. Fig. 5(b) illustrates that in the pulse corona discharge field, the median particle size after agglomeration clearly increased. As input voltage increased and pulse

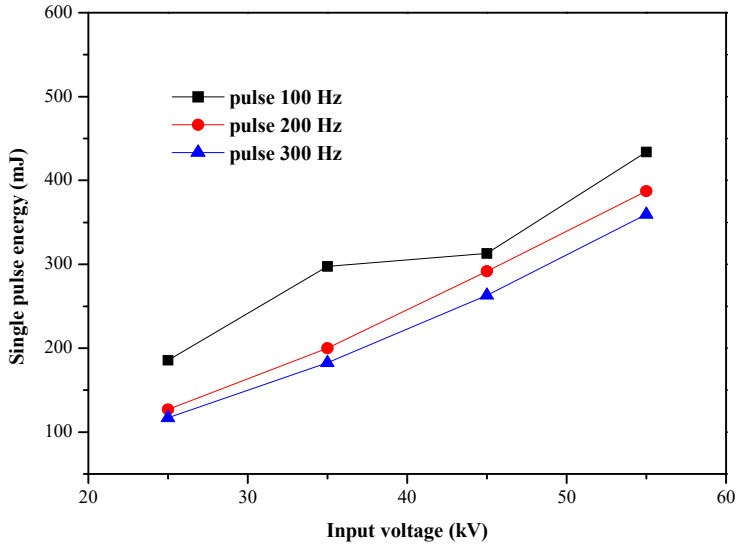

Fig. 4. Influence of the input voltage on the single pulse energy of pulse corona discharge.

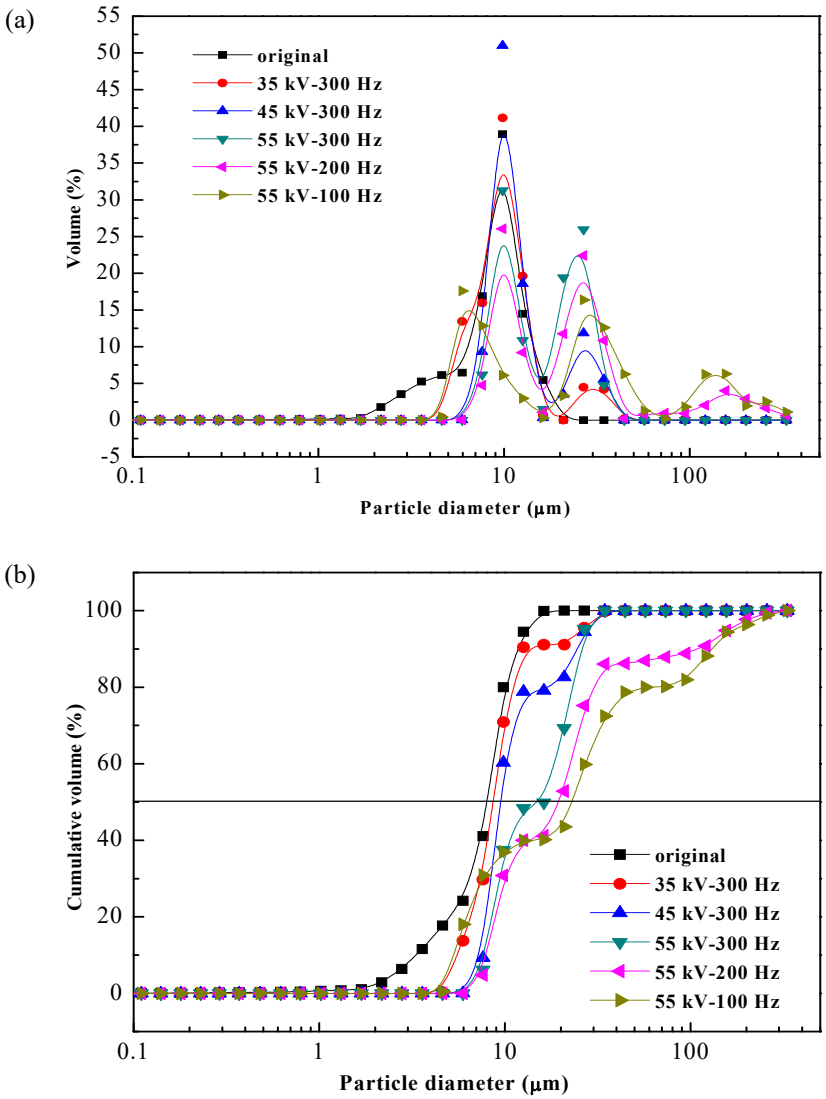

Fig. 5. (a) Volume differential and (b) cumulative distribution of particle size under various pulse input voltages and frequencies.

frequency decreased, D_{50} increased, reaching 23 μm under the condition of 55 kV-100 Hz. Energy input ionized the air and the concentration of high-energy free electrons and ions increased dramatically, which may have increased the intensity of mutual force between charged particles, resulting in easier aggregation of particles.

Agglomeration ratio (R_{ae}) was defined as the ratio of the median particle size after agglomeration to the median size of the original particles. As presented in Fig. 6, when the input voltage was 55 kV, the pulse frequency was 100 Hz; the corresponding median diameter was 23.39 μm; and R_{ae} was 2.93. When the input voltage was increased from 35 to 45 kV, D_{50} and R_{ae} did not exhibit significant changes. This finding suggested that large pulse voltage and low pulse frequency should be selected to maximize the effectiveness of agglomeration within the limits of the experimental conditions.

Effects of Acoustic Wave on the Agglomeration of Fine Particles

In these experiments, because of limits in the experimental conditions, SPLs were 135, 139, and 143 dB. As denoted in Table 1, when SPL was 143dB, both the D_{50} and R_{ae} both first increased and then decreased as the acoustic wave frequency increased. With the decrease of SPL, D_{50} and R_{ae} also decreased. Therefore, the larger the SPL is, the more intense the particle vibration. Additionally, the probability of collision between particles increased and the optimum acoustic frequency was 1600 Hz.

Experiments were performed to investigate the effects of acoustic waves on the agglomeration of fine particles. According to the results of the previously described experiments, SPL = 143 dB was selected. As Fig. 7 presents, the effect of the acoustic frequency on the aggregation of fine particles was complex. When acoustic frequency was 2400 Hz, a new small peak value appeard between 20 and 30 μm. The effects of 800 and 1200 Hz were similar: a wide range of peaks appeared; almost all fine particles agglomerated into large particles; and most particles were 20–80 μm. The frequency of 1600 Hz was most effective for agglomeration; not only did the small particles all agglomerate into large particles but also the peak value was larger than 40 μm after agglomeration. Additionally, obvious peaks were evident at 200 μm. when SPL was

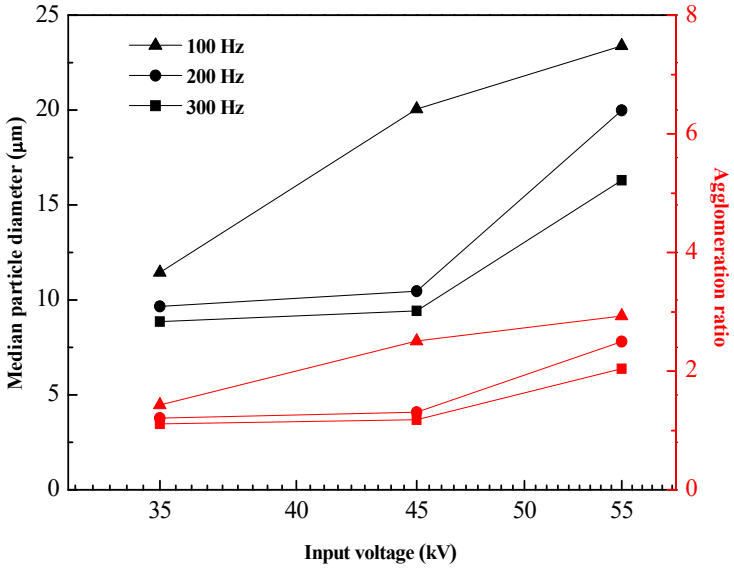

Fig. 6. Median particle diameters and agglomeration ratios of particles under various pulse input voltages and frequencies.

Table 1. Median particle diameters and agglomeration ratios of particles under various acoustic SPLs and frequencies.

frequency	parameters	SPL		
		135dB	139dB	143dB
800 Hz	D_{50}/μm	14.69	24.99	36.88
	R_{ae}	1.84	3.13	4.62
1200 Hz	D_{50}/μm	18.76	27.22	36.95
	R_{ae}	2.35	3.41	4.63
1600 Hz	D_{50}/μm	28.50	41.27	57.56
	R_{ae}	3.57	5.17	7.21
2000 Hz	D_{50}/μm	23.15	26.10	28.10
	R_{ae}	2.90	3.27	3.52
2400 Hz	D_{50}/μm	9.50	15.97	20.52
	R_{ae}	1.19	2.00	2.57

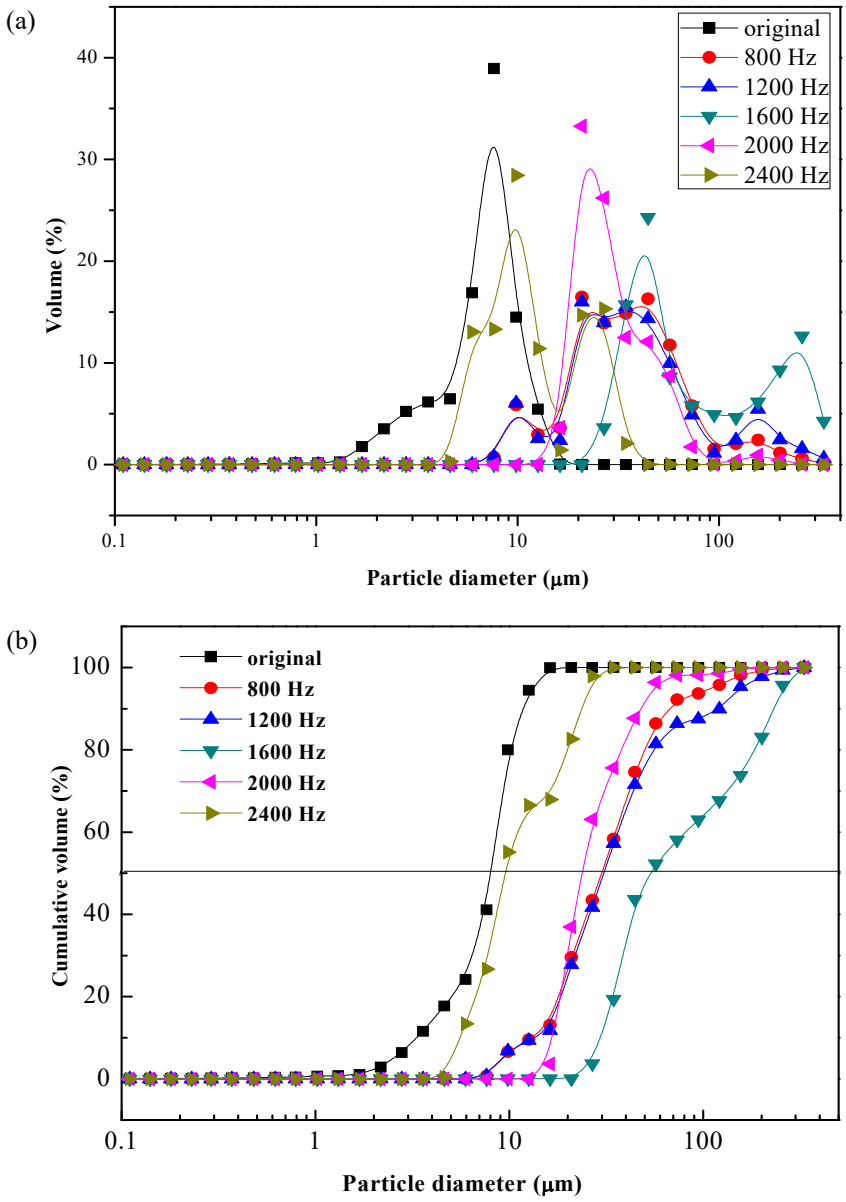

Fig. 7. (a) Volume differential and (b) cumulative distribution under various acoustic wave frequencies (SPL = 143 dB).

143 dB, the acoustic frequency was 1600 Hz; D_{50} of fine particles changed from 7.98 to 57.56 μm, and R_{ae} reached 7.21 (Fig. 8). By contrast, when acoustic frequency was 2400 Hz, D_{50} was only 20.52 μm, and the corresponding R_{ae} was only 2.57. The findings suggested that acoustic frequency should neither be too large nor too small and that optimal frequency value was 1600Hz. Orthokinetic interaction was the predominant mechanism, suggesting that relative movement and collision resulted from differences in the entrainment degrees of particles. If the acoustic frequency was too small, all particles vibrated with the gas medium, and relative motion among particles with different sizes was small. If the acoustic wave frequency was too large, all particles remained still and could not vibrate with the gas medium, and a relative motion effect was not obvious. Therefore, selection of an appropriate acoustic frequency was crucial for ensuring an optimal fine particle agglomeration effect.

Effect of Coupling Field on the Agglomeration of Fine Particles

This experiment was conducted in the acoustic wave and pulse discharge coupling field. The results are presented in Fig. 9. The pulse frequency and voltage were 100 Hz and 55 Kv, respectively, and the acoustic frequency and SPL were 1600 Hz and 143 dB, respectively. The volume proportion of large particles obviously increased, whereas that of fine particles decreased substantially. Most particles with diameters of 9.82 μm were agglomerated into larger particles. The volume proportion of particles with a diameter of 200.68 μm increased to 16.98% in the coupling field and to 1.93% in the pulse corona discharge field. As denoted in Fig. 9(b), D_{50} and R_{ae} significantly increased in the coupling field compared with the single

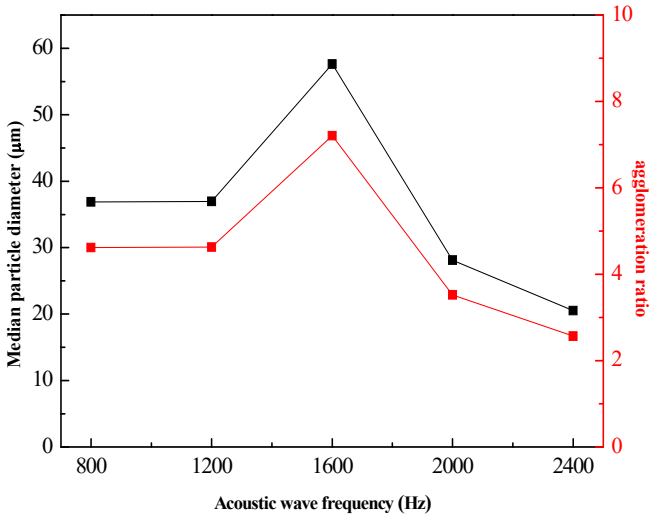

Fig. 8. Median particle diameters and agglomeration ratios of particles under various acoustic wave frequencies (SPL = 143 dB).

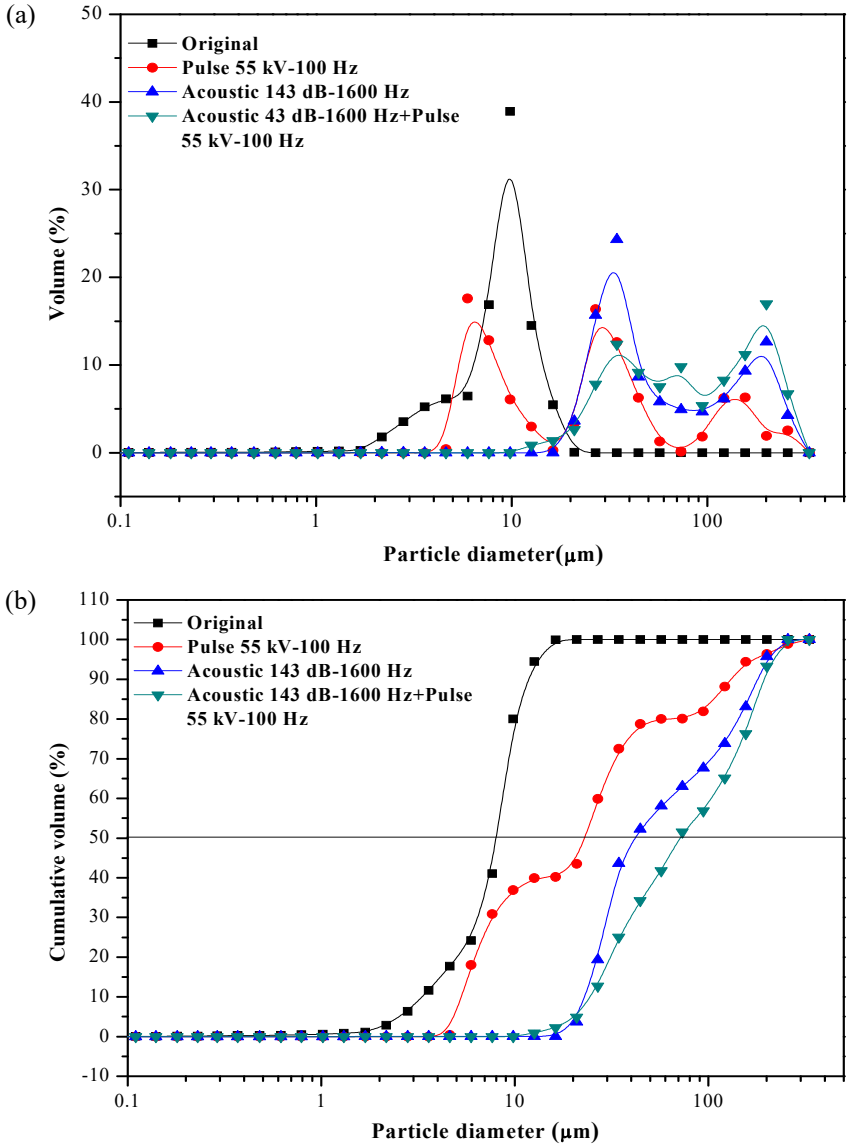

Fig. 9. (a) Volume differential and (b) cumulative distribution of particle size under single field and coupling field.

field, reaching 73.28 μm and 9.18, respectively. Thus, the efficiency of fine particle agglomeration in the coupling field was greater than that of the single field, and D_{50} increased considerably.

Particle Removal Efficiency in Coupling Field

To determine whether agglomeration in the coupling fieldincreased removal efficiency, a laboratory-scale ESP with a negative DC supply was placed at an outlet of the agglomeration chamber. Studies have proven that a negative DC can remove particles efficiently, with the exception of fine particles. In this study, acoustic wave and pulse corona discharge coupling field were used as a pretreatment to force fine particles to agglomerate into larger particles, resulting in significantly more efficient fine particle removal. Removal efficiency was calculated using Eq. (17):

$$\eta = 1 - \frac{N}{N_0} \tag{17}$$

where N_0 is the initial particle number concentration (PNC), and N is PNC at the outlet of the ESP. In this study, the parameters were the same as those used in the previously described agglomeration experiment. DC supply voltage was regulated to 16 kV, which was the highest voltage applied to the ESP in this experiment. As shown in Fig. 10, PNC clearly decreased after particles passed through the ESP. Additionally, the amplitude of PNC decreased less for particles with diameters of 0.15 μm than for those of other sizes. As Fig. 11 illustrates, ESP removal efficiency significantly increased with pretreatment, especially in the coupling field. When only DC supply was applied, removal efficiency was 80.7%, and that of particles with diameters of 0.15 μm was less than 75%.

When particles passed through the agglomeration chamber first, fine particles removal efficiency increased sharply. When the pretreatment was pulse corona discharge, the efficiency increased to approximately 91.6%, and when an acoustic wave field was applied, removal efficiency further increased to 94.4%. Particles with diameters of 0.15 μm were present in the critical area of field charge and diffusion charge; although these particles were difficult to remove, pretreatment resulted in considerable increases in the efficiency of their removal from 75% to 80%, 85%, and 91%. Additionally, overall particle removal efficiency reached 98.3%.

CONCLUSIONS

Comparative experimental studies were conducted to verify the effects of pulse corona discharge and acoustic wave coupling on particle agglomeration and removal efficiency. The coupling field clearly increased agglomeration efficiency when the pulse corona discharge and acoustic wave parameters were 55 kV–100 Hz and 143 dB–1600 Hz, respectively, and D_{50} and R_{ae} values were 11.23 μm, 1.51 and 57.56 μm, 7.21. In the coupling field, the corresponding values increased to 73.28 μm and 9.18, and the effect on agglomeration was obvious. The acoustic wave value of 1600 Hz was optimal for enhancing the agglomeration effect, and when the SPL value rose, agglomeration efficiency increased in response. When pulse frequency was 100 Hz, the single pulse energy injection reached its maximum, and more fine particles were charged and aggregated into larger particles. Under the acoustic wave and pulse corona discharge coupling field, overall removal efficiency reached 98.3%, and particles with diameters of 0.15 μm were in the critical area of field charge and diffusion charge. Although these particles were difficult to remove, the grade removal efficiency substantially improved, from 75.1% to 80%, 85.3%, and 91.4%. Finally, the coupling field was more effective than the single field as a pretreatment for fine particle.

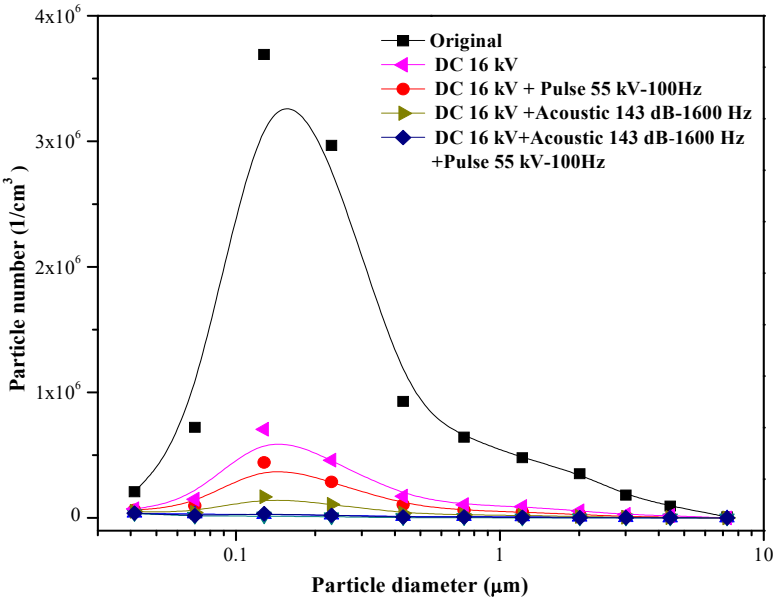

Fig. 10. Comparison of particle number distribution after ESP under various pretreatment conditions.

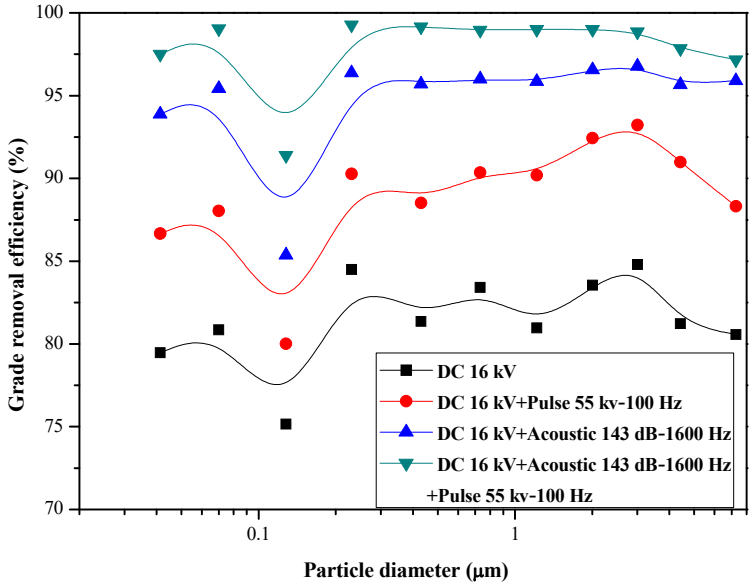

Fig. 11. Grade removal efficiency of fine particles after application of ESP with single field and coupling field.

ACKNOWLEDGEMENTS

This work was supported from the National Basic Research Program (973) of China (No. 2013CB228504). This manuscript was edited by Wallace Academic Editing.

REFERENCES

Bates, D.R., Massey, H.S.W. and Amdur, I. (1962). Atomic and molecular processes. *Phys. Today* 15: 63–63.

Chen, C.C., Tao, C.J. and Cheng, H.C. (2002). Condensation of supersaturated water vapor on charged/neutral nanoparticles of glucose and monosodium glutamate. *J. Colloid Interface Sci.* 255: 158–170.

Chen, H., Wang, T., Luo, Z., Zhou, D., Lu, M., He, M., Fang, M. and Cen, K. (2017). Agglomeration kernel of bipolar charged particles in the presence of external acoustic and electric fields. *Aerosol Air Qual. Res*. 17: 857–866.

Fan, F., Yang, X. and Chang, N.K. (2013). Direct simulation of inhalable particle motion and collision in a standing wave field. *J. Mech. Sci. Technol.* 27: 1707–1712.

Hoffmann, T.L. (2000). Environmental implications of acoustic aerosol agglomeration. *Ultrasonics* 38: 353.

Jiang, J.P., Luo, Z.Y., Chen, H., Zhou, D., Sha, D.H., Fang, M.X. and Cen, K.F. (2015). Orthogonal design process optimization for particle charge distribution of mosquito coil smoke aerosol enhanced by pulsed corona discharge. *Powder Technol.* 286: 507–515.

Le, T.C., Lin, G.Y. and Tsai, C.J. (2013). The predictive method for the submicron and nano-sized particle collection efficiency of multipoint-to-plane electrostatic precipitators. *Aerosol Air Qual. Res*. 13: 1404–1410.

Liao, Z., Li, Y., Xiao, X., Wang, C., Cao, S. and Yang, Y. (2018). Electrostatic precipitation of submicron particles with an enhanced unipolar pre-charger. *Aerosol Air Qual. Res*. 18: 1141–1147.

Liu, B.Y.H. and Kapadia, A. (1978). Combined field and diffusion charging of aerosol particles in the continuum regime. *J. Aerosol Sci.* 9: 227–242.

Liu, J., Zhang, G., Zhou, J., Wang, J., Zhao, W. and Cen, K. (2009). Experimental study of acoustic agglomeration of coal-fired fly ash particles at low frequencies. *Powder Technol.* 193: 20–25.

Liu, J., Wang, J., Zhang, G., Zhou, J. and Cen, K. (2011). Frequency comparative study of coal-fired fly ash acoustic agglomeration. *Res. J. Environ. Sci.* 23: 1845–1851.

Liu, J.X., Gao, J.H., Gao, J.M., Wang, X.F. and Wu, S.H. (2009). Agglomeration of particles during coal combustion in multistage spouted fluidized tower. *Korean J. Chem. Eng.* 26: 907–912.

Luo, Z., Chen, H., Wang, T., Zhou, D., Lu, M., He, M., Fang, M. and Cen, K. (2017). Agglomeration and capture of fine particles in the coupling effect of pulsed corona discharge and acoustic wave enhanced by spray droplets. *Powder Technol.* 312: 21–28.

Matsoukas, T. (1997). The coagulation rate of charged aerosols in ionized gases. *J. Colloid Interface Sci.* 187: 474–483.

McAdams, R. (2007). Pulsed corona treatment of gases: System scaling and efficiency. *Plasma Sources Sci. Technol.* 16: 703.

O'Hara, D.B., Clements, J.S., Finney, W.C. and Davis, R.H. (1989). Aerosol particle charging by free electrons. *J. Aerosol Sci.* 20: 313–330.

Sheng, C. and Shen, X. (2007). Simulation of acoustic agglomeration processes of poly-disperse solid particles. *Aerosol Sci. Technol.* 41: 1–13.

Wang, J., Liu, J., Zhang, G., Zhou, J. and Cen, K. (2011). Orthogonal design process optimization and single factor analysis for bimodal acoustic agglomeration. *Powder Technol.* 210: 315–322.

Wang, Y., Cheng, K., Tian, H.Z., Yi, P. and Xue, Z.G.

(2016). Emission characteristics and control prospects of primary $PM_{2.5}$ from fossil fuel power plants in China. *Aerosol Air Qual. Res.* 16: 3290–3301.

Xu, F., Luo, Z., Bo, W., Zhao, L., Gao, X., Fang, M. and Cen, K. (2009). Experimental investigation on charging characteristics and penetration efficiency of $PM_{2.5}$ emitted from coal combustion enhanced by positive corona pulsed ESP. *J. Electrostat.* 67: 799–806.

Xu, P., Wang, W., Ji, J. and Yao, S. (2014). Analysis of the contribution of the road traffic industry to the $PM_{2.5}$ emission for different land-use types. *Comput. Intell. Neurosci.* 2014: 821973.

Yan, J., Chen, L. and Yang, L. (2016). Combined effect of acoustic agglomeration and vapor condensation on fine particles removal. *Chem. Eng. J.* 290: 319–327.

Zhang, G.X., Liu, J.Z., Wang, J., Zhou, J.H. and Cen, K.F. (2012). Numerical simulation of acoustic wake effect in acoustic agglomeration under Oseen flow condition. *Chin. Sci. Bull.* 57: 2404–2412.

Zhang, G., Zhang, L., Wang, J. and Hu, E. (2017). Improving acoustic agglomeration efficiency by addition of sprayed liquid droplets. *Powder Technol.* 317: 181–188.

Zhou, C.H., Gong, S., Zhang, X.Y., Liu, H.L., Xue, M., Cao, G.L., An, X.Q., Che, H.Z., Zhang, Y.M. and Niu, T. (2012). Towards the improvements of simulating the chemical and optical properties of Chinese aerosols using an online coupled model – CUACE/Aero. *Tellus B* 64: 91–102.

Zhou, D., Luo, Z., Fang, M., Lu, M., Jiang, J., Chen, H. and He, M. (2016a). Numerical calculation of particle movement in sound wave fields and experimental verification through high-speed photography. *Appl. Energy.* 185: 2245–2250.

Zhou, D., Luo, Z., Jiang, J., Chen, H., Lu, M. and Fang, M. (2016b). Experimental study on improving the efficiency of dust removers by using acoustic agglomeration as pretreatment. *Powder Technol.* 289: 52–59.

Received for review, September 22, 2018
Revised, May 5, 2019
Accepted, September 3, 2019